

NUMERICAL ANALYSIS OF THE INTAKE VORTEX FORMATION IN THE CASE OF A DOUBLE FUSELAGE SHIELDED INLET

ADAM KOZAKIEWICZ, MICHAŁ FRANT

Military University of Technology, Faculty of Mechatronics and Aviation, Warsaw, Poland

e-mail: adam.kozakiewicz@wat.edu.pl; michal.frant@wat.edu.pl

The paper raises a very important problem, concerning the work of turbine-jet engines, that is the intake vortex. A phenomenon which is relevant to all engines of this type. The article demonstrates literature data determining the influence of the airflow direction and zone on the possibility of vortex formation, taking into consideration the influence of basic geometrical data. The outcomes of calculations related to the formation of the inlet vortex for a given fuselage shielded inlet constructional system are shown. The studies are concerned with determination of the influence of angles and the gust speed value on forming of the vortex in this kind of intake.

Keywords: turbine-jet engine, inlet intake vortex, computational fluid dynamics

1. Introduction

In the case of turbine-jet engines, a vortex often happens to form in the intake system of the engine (Fig. 1). The phenomenon takes place when an engine works on the ground. Rotary movement of the air itself is connected to the air particles rotating with a certain angular speed which finally form a vortex tube, characterized by a stagnation line and a stagnation point (Hirsch, 2007; Kazimierski, 2004, 2007). Burgers, Lamba-Oseen, Rankin and Vatistas's models are used to describe the vortex phenomenon, the two most important parameters in those models are: radius of the vortex as well as the tangential speed. The process of vortex formation in the inlet system is dependent on the engine thrust (mass flow), speed, and direction of the wind flow as well as the intake diameter and height of its location.



Fig. 1. Vortex (marked with an arrow) in the inlet system of the F117-PW-100 (PW2040) engine on a C-17 aircraft

Determination of the base of a vortex (distance from central line), in the case of a subsonic inlet system, depends on geometrical parameters (Fig. 2), including relations between the level

of inlet lip H and inlet diameter D . To create this type of characteristics, non-dimensional parameters in form of a combination of geometrical parameters are used. It permits one generalize conclusions, regarding the whole group of engine inlets, in terms of susceptibility of vortex creation or lack of it, with regard to the angular direction of the flow and zones of headwind and tailwind.

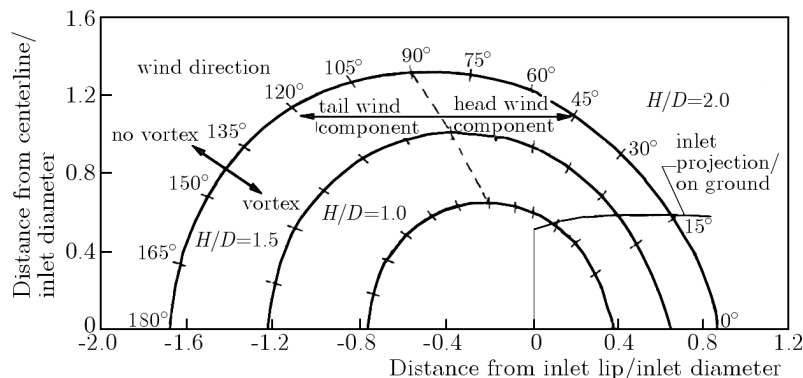


Fig. 2. The stagnation point function vs. constructional parameters of the inlet (Motycka *et al.*, 1973)

The aim of the article is to show the outcomes concerning this type of issues related to influence of the change in the gust direction and the value of speed on creation of vortex for the existing structural systems.

2. Building the computational grid

To build a virtual model of a fuselage shielded inlet, the structural solution of an aircraft MiG-29 was used. Using the reverse engineering method (Kachel and Kozakiewicz, 2012; Kachel *et al.*, 2011) the inlet geometry model was made. One used Unigraphics system to design the geometry of the aircraft inlet. The following was required for calculation by the FLUENT package in the given stages:

- import of the solid from an external CAD program file,
- choice of the computational region,
- assessment of acceptability and possibility of simplifying the object for numerical analysis,
- discretization of the inlet model of the studied object as well as discretization of the computational domain,
- formulation of boundary conditions and exporting them to the solver.

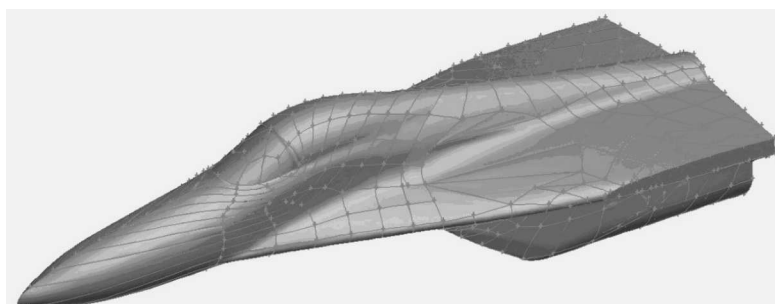


Fig. 3. Computational model of a double fuselage shielded inlet

Figure 3 depicts a model of a double fuselage shielded inlet imported to the Gambit pre-processor. On the external surface, the object holds a series of small surfaces comparing to

the rest. Those, quite considerably, complicate the process of building the surface grid on the computational model. It originated the need for conducting an operation called clearing the geometry.

A considerable issue on the level of constructing the computational model is determination of the domain, which affects calculation time and precision. This parameter was chosen basing on the gained experiences from similar studies (Kozakiewicz and Frant, 2011, 2013). In this case, the computational domain assumes a form of cuboid measuring $20\text{ m} \times 10\text{ m} \times 10\text{ m}$. The virtual object has been placed in such a way that the nose of the fuselage is found at the beginning of the coordinates system. Next, a smaller domain of $10\text{ m} \times 5\text{ m} \times 3.8\text{ m}$, in which the studied object is placed, was sectioned (Fig. 4) out of the bigger one. Thanks to that effort, in the internal domain the grid is thicker, what is important considering the accuracy of calculations. Inside the remaining zone, the grid system is thinner, because there is no such big lapse in the parameters.

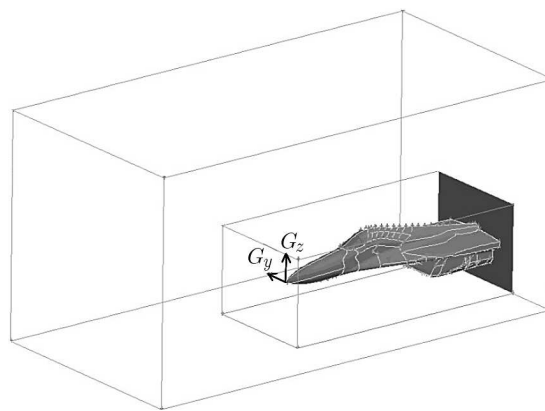


Fig. 4. View of the calculations domain with a separated subdomain

After merging smaller surfaces into bigger ones, it became possible to streamline the process of building the surface grid. Discretized surfaces defining the studied object are presented in Fig. 5. Regarding the geometrical complexity of the object, a triangular surface grid was used.

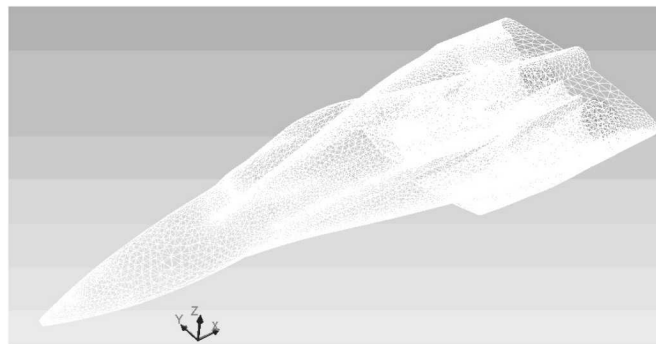


Fig. 5. View to the surface discretization of the studied object

Internal surfaces defining the internal subdomain and external surface were discretized using triangular grids (Fig. 6.). After discretizing all the surfaces, the computational domain was discretized. Tetrahedral elements were used for that. This way the constructed grid adds up to 1 350 000 finite volumes.

Imposed boundary conditions involve side as well as upper surfaces of the external domain, which is limited by the pressure far field condition. The wall condition was imposed on the lower surface of the external domain that constitutes the base. The surfaces determining the studied

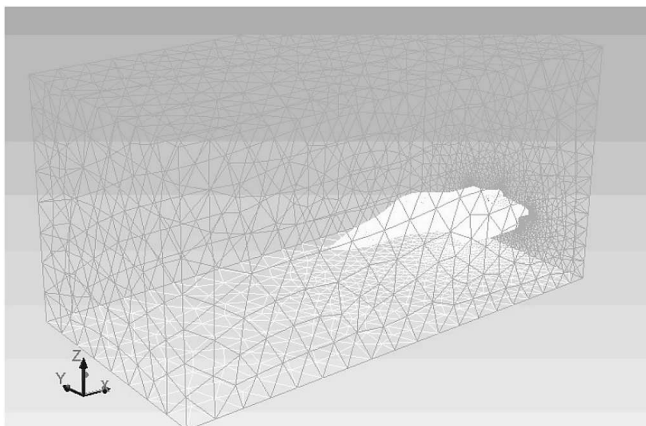


Fig. 6. View to the discretization of the external zone

object also have the imposed wall condition. On the surfaces determining inlets of the engines compressors, the outlet condition was imposed. This way, a computational pattern emerged, used for analysis in the FLUENT environment, in which the calculations were carried out.

3. Numerical analysis of the inlet vortex phenomenon

This part of the article presents the outcomes of numerical analysis of possible inlet vortex formation on the RD-33 engine inlet system model in a MiG-29 airplane. Tested examples have the airplane stranded to examine the impact of the wind direction as well as its speed on forming an inlet vortex. Calculations have been done for the cases of change in the gust for numbers $Ma = 0.0025$ (cr. 0.87 m/s), $Ma = 0.005$ (1.73 m/s), $Ma = 0.0075$ (2.60 m/s), $Ma = 0.01$ (3.47 m/s), and $Ma = 0.015$ (5.21 m/s). In addition, the angle of the gust impact was being changed, its values were accepted as $\alpha = 0^\circ, -5^\circ, -10^\circ, -15^\circ$ (angles on the XZ surface – Fig. 7) and angles $\beta = 0^\circ, 15^\circ, 30^\circ, 45^\circ, 60^\circ, 90^\circ$ (angles on the XY surface – Fig. 7). It all added up to a total of 130 computational cases.

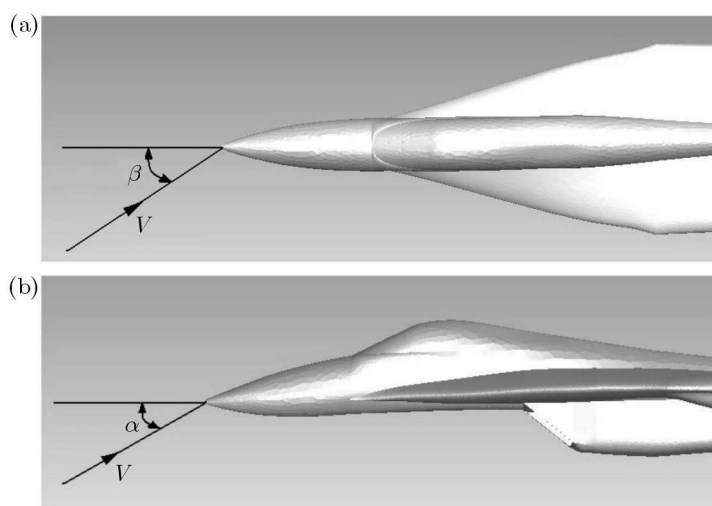


Fig. 7. Determining the α and β angles

The first computational case is a gust with speed of $Ma = 0.0025$ (0.87 m/s). The outcomes are presented in Table 1. Within the whole range of gust angles $\beta = 0^\circ, \dots, 90^\circ$ and

$\alpha = 0^\circ, \dots, 15^\circ$ the vortex appeared either on one or both inlets. In the case of a frontal gust, if $\beta = 0^\circ$ (Fig. 8), the vortex appears on both ducts for every variant of change in the angle of gust α (angle on the surface xz).

Table 1. Gust with speed of $Ma = 0.0025$ (0.87 m/s)

	$\beta = 0^\circ$	$\beta = 15^\circ$	$\beta = 30^\circ$	$\beta = 45^\circ$	$\beta = 60^\circ$	$\beta = 90^\circ$
$\alpha = 0^\circ$	++	+-	+-	+-	+-	-+
$\alpha = -5^\circ$	++	+-	+-	+-	+-	++
$\alpha = -10^\circ$	++	+-	+-	+-	++	++
$\alpha = -15^\circ$	++	+-	+-	++	++	++

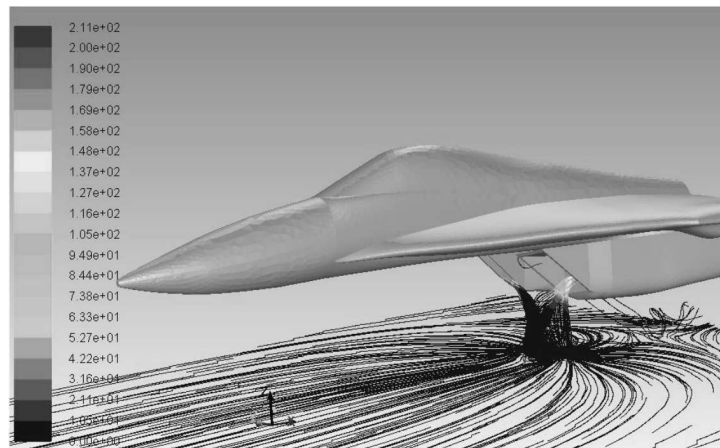


Fig. 8. Streamlines for $Ma = 0.0025$, $\beta = 0^\circ$, $\alpha = 0^\circ$

The change in the direction of the β gust on the xy surface first led to the disappearance of a vortex in the left inlet duct (computational case $\beta = 15^\circ, 30^\circ$ – Fig. 9) – in the whole range of change of the α angle. The second, after a shift to $\beta = 45^\circ$ vortices reappeared on both ducts with the angle α being at its maximum. Subsequent increasing of the angle β led to obtaining vortices on both ducts, range of the angle $\beta = 90^\circ$. Exception for the $\alpha = 0^\circ$ condition, the phenomenon is presented on an exemplary computational outcome for the angles $\beta = 90^\circ$ and $\alpha = -15^\circ$ (Fig. 10).

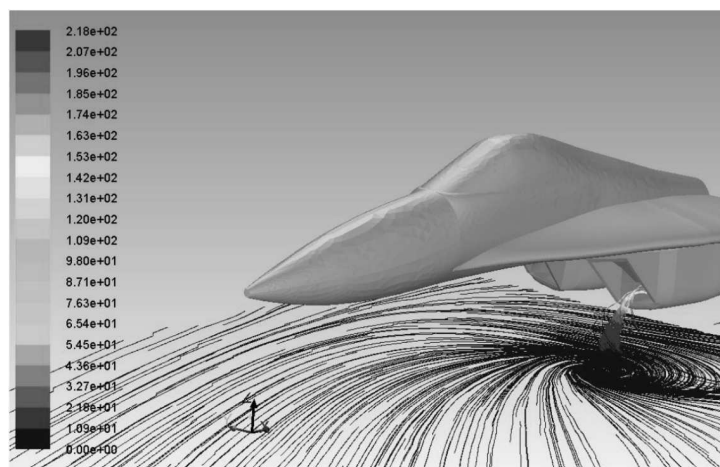


Fig. 9. Streamlines for $Ma = 0.0025$, $\beta = 30^\circ$, $\alpha = -10^\circ$

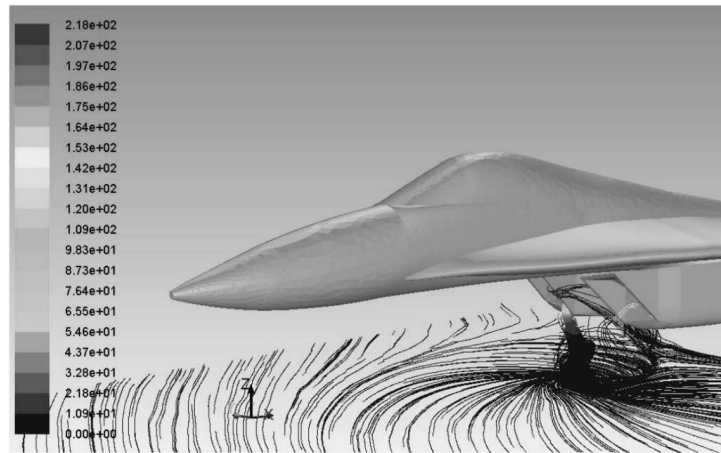


Fig. 10. Streamlines for $Ma = 0.0025, \beta = 90^\circ, \alpha = -15^\circ$

Another computational case corresponding to the growth of the Mach number to a value of $Ma = 0.005$ (1.73 m/s), in the same field of change in the gust angle α and β (Table 2), led to the appearance of vortexes only for $\beta = 0^\circ$ in the whole range of studied changes in the α angle. The outcomes for a neutral range for β angle and $\alpha = -10^\circ$ is shown in Fig. 11. The increase in the β angle ($\beta = 15^\circ, \dots, 90^\circ$), just as in the first case, leads to the disappearance of the vortex in the left inlet (see Fig. 12). The sum of the impact of the gust force and impact of the second duct causes the right duct vortex to last. Increasing the β angle, again does not cause the appearance of a vortex on both ducts, as it is in the case of $Ma = 0.0025$ gust, which is very well visible on the attached outcomes (Fig. 13).

Table 2. Gust with a $Ma = 0.005$ (1.73 m/s) speed

	$\beta = 0^\circ$	$\beta = 15^\circ$	$\beta = 30^\circ$	$\beta = 45^\circ$	$\beta = 60^\circ$	$\beta = 90^\circ$
$\alpha = 0^\circ$	++	-+	-+	-+	-+	-+
$\alpha = -5^\circ$	++	-+	-+	-+	-+	-+
$\alpha = -10^\circ$	++	-+	-+	-+	-+	-+
$\alpha = -15^\circ$	++	-+	-+	-+	-+	-+

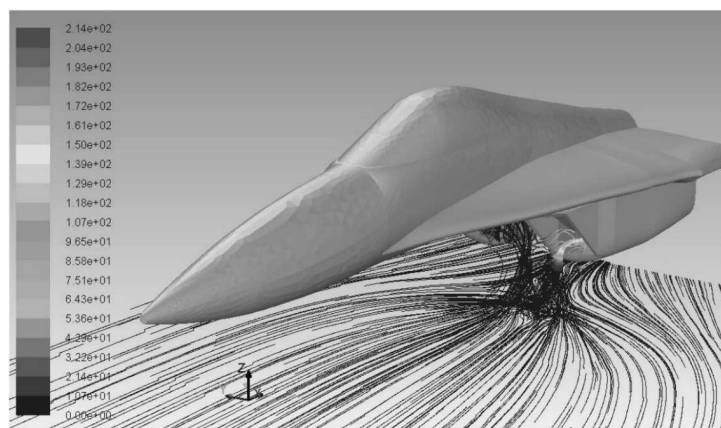
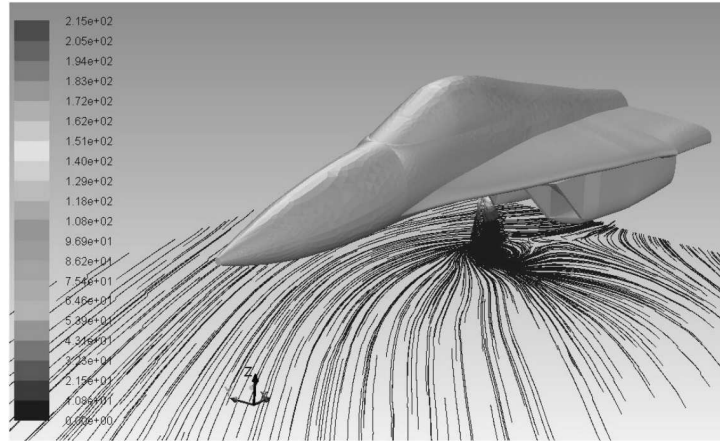
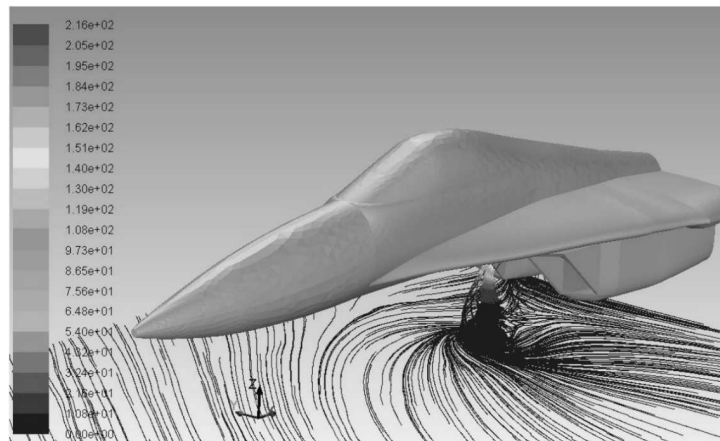


Fig. 11. Streamlines for $Ma = 0.005, \beta = 0^\circ, \alpha = -10^\circ$

A further case connected to the growth of a gust value to $Ma = 0.0075$ (2.60 m/s) caused a restriction on the gust angles range enabling formation of vortexes not only on one, but both inlet ducts. The outcomes are presented in Table 3. However, in the case of weaker flows, that is


 Fig. 12. Streamlines for $Ma = 0.005$, $\beta = 30^\circ$, $\alpha = -10^\circ$

 Fig. 13. Streamlines for $Ma = 0.005$, $\beta = 90^\circ$, $\alpha = 0^\circ$
Table 3. Gust with a speed of $Ma = 0.0075$ (2.60 m/s)

	$\beta = 0^\circ$	$\beta = 15^\circ$	$\beta = 30^\circ$	$\beta = 45^\circ$	$\beta = 60^\circ$	$\beta = 90^\circ$
$\alpha = 0^\circ$	+-	++	-+	-+	--	-+
$\alpha = -5^\circ$	+-	++	-+	-+	--	-+
$\alpha = -10^\circ$	--	++	-+	--	--	-+
$\alpha = -15^\circ$	--	-+	--	--	--	--

$Ma = 0.0025$ and 0.005 as well as frontal airflow (angle $\beta = 0^\circ$) vortices were obtained on both ducts, yet, researching this speed, the vortex was obtained on a single duct, and with a limited range of the angle α ($\alpha = 0^\circ$; -5°). Conditions facilitating generation of vortices on both ducts were only obtained with $\beta = 15^\circ$ (Fig. 14) except for $\alpha = -15^\circ$, which led to disappearance of the vortex on the left inlet. Consequent growth of the β angle causes a shift to one vortex (Fig. 15), except for the flow with an angle of $\alpha = -15^\circ$ which did not lead to vortex formation on both ducts just as for $\alpha = -10^\circ$ and $\beta = 45^\circ$ (Fig. 16) and $\beta = 30^\circ$ case.

The last stage of calculations (Table 4) has been carried out while raising the speed of airflow to a value of $Ma = 0.01$ (3.47 m/s). This caused a nearly complete disappearance of the vortex, presented in Fig. 17 and Fig. 19. Only in the case of $\beta = 30^\circ$ and $\alpha = 0^\circ$ a vortex was obtained, only on one inlet as presented in Fig. 18. This level of speed eliminates the possibility of vortex formation.

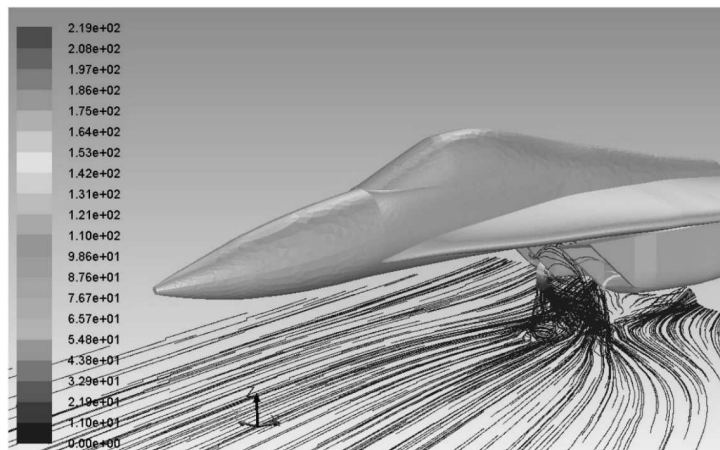


Fig. 14. Streamlines for $Ma = 0.0075, \beta = 15^\circ, \alpha = -10^\circ$

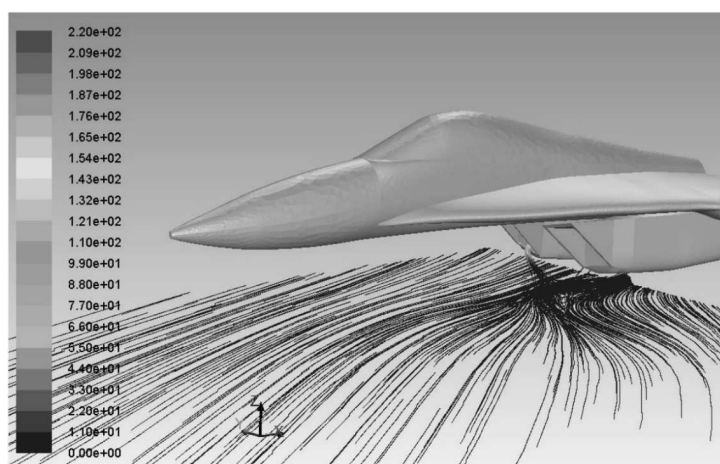


Fig. 15. Streamlines for $Ma = 0.0075, \beta = 30^\circ, \alpha = -10^\circ$

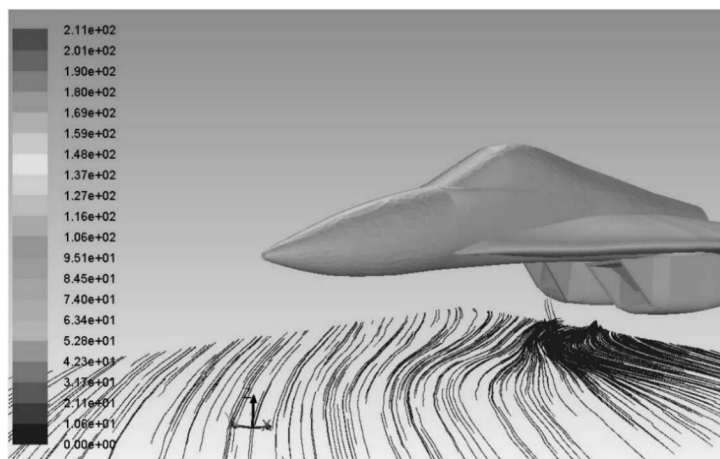


Fig. 16. Streamlines for $Ma = 0.0075, \beta = 45^\circ, \alpha = -10^\circ$

Table 4. Gust with a speed of $Ma = 0.01$ (3.47 m/s)

	$\beta = 0^\circ$	$\beta = 15^\circ$	$\beta = 30^\circ$	$\beta = 45^\circ$	$\beta = 60^\circ$	$\beta = 90^\circ$
$\alpha = 0^\circ$	---	---	--+	---	---	---
$\alpha = -5^\circ$	---	---	---	---	---	---
$\alpha = -10^\circ$	---	---	---	---	---	---
$\alpha = -15^\circ$	---	---	---	---	---	---

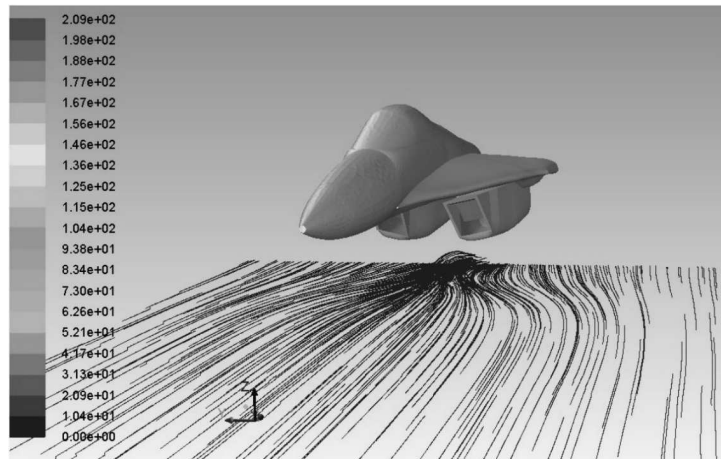


Fig. 17. Streamlines for $Ma = 0.01, \beta = 0^\circ, \alpha = 0^\circ$

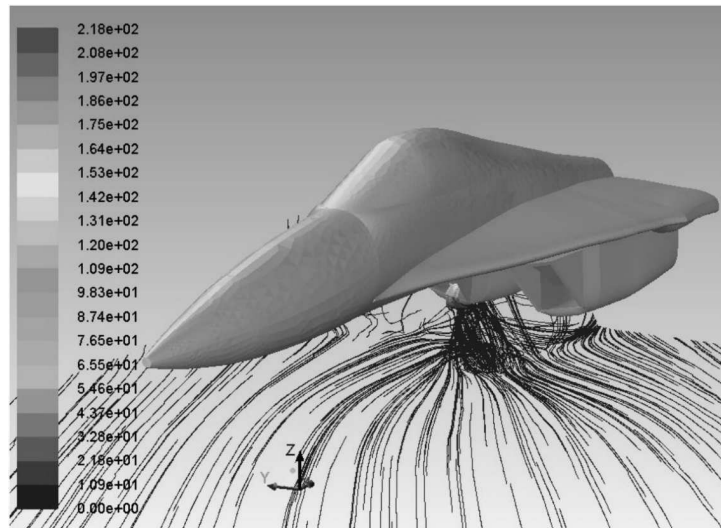


Fig. 18. Streamlines for $Ma = 0.01, \beta = 30^\circ, \alpha = 0^\circ$

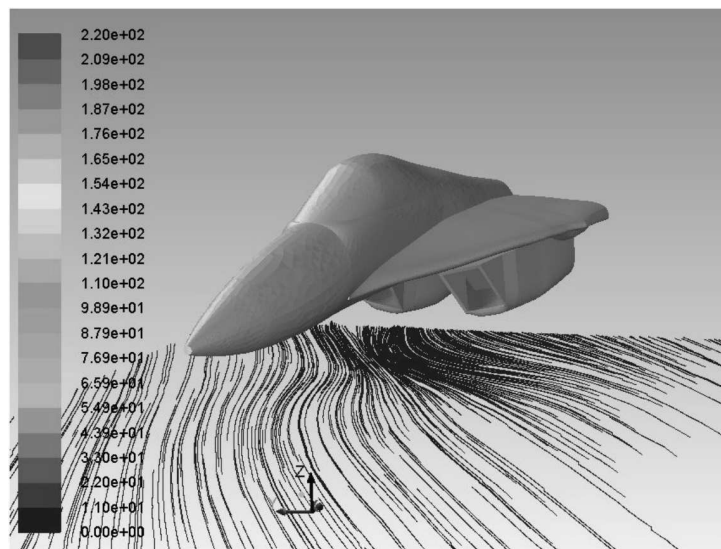


Fig. 19. Streamlines for $Ma = 0.01, \beta = 30^\circ, \alpha = -10^\circ$

The last computational case deals with calculations for a gust speed of $Ma = 0.015$ (5.21 m/s) to examine the disappearance of vortexes at higher speeds. Data obtained from numerical calculations concerning the possibility of vortex formation has been gathered in Table 5. It is clear that this level of gust did not form a vortex in any case, neither in the double order for both inlets nor in the single one for any inlet.

Table 5. Gust for $Ma = 0.015$ (5.21 m/s)

	$\beta = 0^\circ$	$\beta = 15^\circ$	$\beta = 30^\circ$	$\beta = 45^\circ$	$\beta = 60^\circ$	$\beta = 90^\circ$
$\alpha = 0^\circ$	---	---	---	---	---	---
$\alpha = -5^\circ$	---	---	---	---	---	---
$\alpha = -10^\circ$	---	---	---	---	---	---
$\alpha = -15^\circ$	---	---	---	---	---	---

4. Summary

As a result of the conducted numerical analysis, the possibility of vortex formation simultaneously on both inlet ducts of an aircraft was proven. In this case, the less advantageous condition is a frontal airflow for $Ma = 0.0025$ and 0.0075 . Next, the largest group of vortexes on both inlets was obtained for a flow with $Ma = 0.0075$ and the angle $\beta = 15^\circ$. The growth of the gust speed leads to a transfer of the vortex form the left to the right duct. Formation of vortexes was always confirmed using small airflows. Growing speed of gust prevents an inlet vortex from forming – already speed of $Ma = 0.01$ (3.47 m/s) leads to the lack of vortexes, apart from one case ($\beta = 30^{circ}$ and $\alpha = 0^\circ$).

References

1. HIRSCH C., 2007, *Numerical Computation of Internal and External Flows, Fundamentals of Computational Fluid Dynamics*, 2nd Edition, Elsevier
2. KOZAKIEWICZ A., FRANT M., 2011, Development of a model for the intake system of the F-100-PW-229 engine for the F-16 aircraft in order to analyze formation of a intake vortex (in Polish), *Prace Instytutu Lotnictwa*, **213**, 55-65
3. KOZAKIEWICZ A., FRANT M., 2013, The analysis of the gust impact on inlet vortex formation of fuselage-shielded inlet of a jet engine powered aircraft, *Journal of Theoretical and Applied Mechanics*, **51**, 4, 993-1002
4. KACHEL S., KOZAKIEWICZ A., 2012, Application of the reverse engineering to the modelling of intake channel of MRCA turbine engine for the use of flow research (in Polish), *Biuletyn WAT*, **LXI**, 2(666), 311-330
5. KACHEL S., KOZAKIEWICZ A., ŁĄCKI T., OLEJNIK A., 2011, The use of reverse engineering for the process of reproducing the geometry of the configuration of the intake-engine RD-33 in a MiG-29 aircraft (in Polish), *Prace Instytutu Lotnictwa, Zagadnienia napędów lotniczych*, **213**, 66-84
6. KAZIMIERSKI Z., 2004, *Fundamentals of Fluid Mechanics and Methods of Flow Computational Simulation* (in Polish), Politechnika Łódzka, Łódź
7. KAZIMIERSKI Z., 2007, *Rotational Motion of Fluids in Nature and in Machinery and Equipment* (in Polish), Politechnika Łódzka, Łódź
8. MOTYCKA D., WALTER W., MULLER G., 1973, An analytical and experimental study of inlet ground vortices, *AIAA Paper, AIAA/SAE 9th Propulsion Conference*, **No. 73/1313**